

Vugt N. van, Bruijn H. de, Kolfshoten M. van & Langereis C.G.

Magneto- and cyclostratigraphy and
mammal-fauna's of the Pleistocene lacustrine
Megalopolis Basin, Peloponnesos, Greece

pp. 69-92, 2 Pls, 6 figs.

Magneto- and cyclostratigraphy and mammal-fauna's of the Pleistocene lacustrine Megalopolis Basin, Peloponnesos, Greece

Abstract

The Pleistocene Megalopolis basin contains lacustrine silt, clay and marl with regularly intercalated lignite seams. Mammal fauna's that were collected from four levels indicate a late Early to Late Biharian age (middle Pleistocene). The magnetostratigraphic study revealed the Matuyama-Brunhes boundary in the section. Reversal excursions were not recorded or indistinguishably overprinted by delayed acquisition of magnetic remanence.

The regular pattern of lignite seams is argued to be related to 100 kyr eccentricity, with the lignite intervals corresponding to eccentricity maxima. Smaller-scale lignite cycles are correlated to insolation maxima. This interpretation leads to the conclusion that organic material was preserved during warm and humid periods, while predominantly detrital material was deposited during relatively cool and dry intervals.

Generally, $\delta^{18}\text{O}$ minima correspond to eccentricity maxima in the Pleistocene. However, the interglacial oxygen isotope stages 19 and 11, which correspond to very low-amplitude eccentricity maxima, have a normal amplitude. Interestingly, the pattern of lignite seams in Megalopolis corresponds much better to the eccentricity curve than to the $\delta^{18}\text{O}$ record. This suggests that environmental/climatic changes on the Mediterranean continent are forced by a mechanism different from the one that forces glaciations as reflected by marine $\delta^{18}\text{O}$ records.

Introduction

Sediments are a natural archive for the Earth's climate. The many studies on Mediterranean sedimentary sections have provided a wealth of palaeoclimatic information. A multi-disciplinary research programme on continental-marine correlations in the Mediterranean aims to study different non-marine Neogene sedimentary environments. High-resolution time frames for such deposits, established through correlation with marine reference sections and/or astronomical target curves, are the basis for various detailed studies that enhance our understanding of the coupling between astronomical parameters, palaeoclimate and palaeoenvironment in different realms. Miocene floodplain and distal alluvial environments from the western Mediterranean are currently being investigated (Abdul Aziz et al., 2000; Krijgsman et al., 1994), as well as a Pliocene shallow lacustrine carbonate-lignite system from northern Greece (Steenbrink et al., 1999; van Vugt et al., 1998). A study on much younger (Pleistocene) lacustrine deposits is presented here.

The lignite-containing lacustrine sediments in the Megalopolis basin have been studied for geological and mining purposes since 1962 (Lüttig and Marinos, 1962; Vinken, 1965). More recently, various studies in the Megalopolis lignite mines have contributed to the Pleistocene palaeoclimate records (Benda et al., 1987; Nickel et al., 1996, among others). The detailed study by Nickel et al. suggests that lignites were formed during an interglacial or interstadial, thus hinting at a cyclic origin for the groups of lignite seams. The present study aims at identifying such a cyclic origin, finding the periodicity and correlating the cycles to an astronomical solution. Palaeontology and magnetostratigraphy provide the first-order time control.

Geological background

The intramontane lacustrine Megalopolis Basin is located in the middle of the Peloponnesos peninsula in southern Greece (Figure 1), at the boundary between Mesozoic limestones of the Pindos zone and Eocene flysch of the Tripolitza Group (Vinken, 1965). The eastern margin of the basin is formed by NE-SW trending normal faults, that have been active since the Late Miocene.

Upper Pliocene lacustrine and fluvial units overly the limestone and flysch basement, followed by Pleistocene fluvial conglomerates of the Apiditsa Formation in the western and central part of the basin (Figure 1). The overlying Choremi Formation, especially its Marathousa Member, with lacustrine clay, silt, lignite, and some sand beds in the centre of the basin, and fluvial sediments at the margins is of main interest to this study. Fluvial terraces and braided channel deposits constitute the top of the Pleistocene basin fill (Vinken, 1965).

Three open pit lignite mines provide large, unweathered exposures of the Marathousa Member. The lignite has previously been divided into three major coal seams (Löhnert and Nowak, 1965), divided by clay, silt and sand partings of 5–30 m thick. This classifi-

cation is in close agreement with the cyclic pattern distinguished in the Marathousa member (see below). Based on this cyclic interpretation, we prefer to arrange the lignite seams into four groups: I-IV (Figure 2), of which groups III and IV belong to Löhnert's uppermost (Panagiatis) group.

The lignite layers exposed in the mines are thickest in the western part of the mines and wedge out towards the east, as opposed to the detrital layers, that are thickest in the east

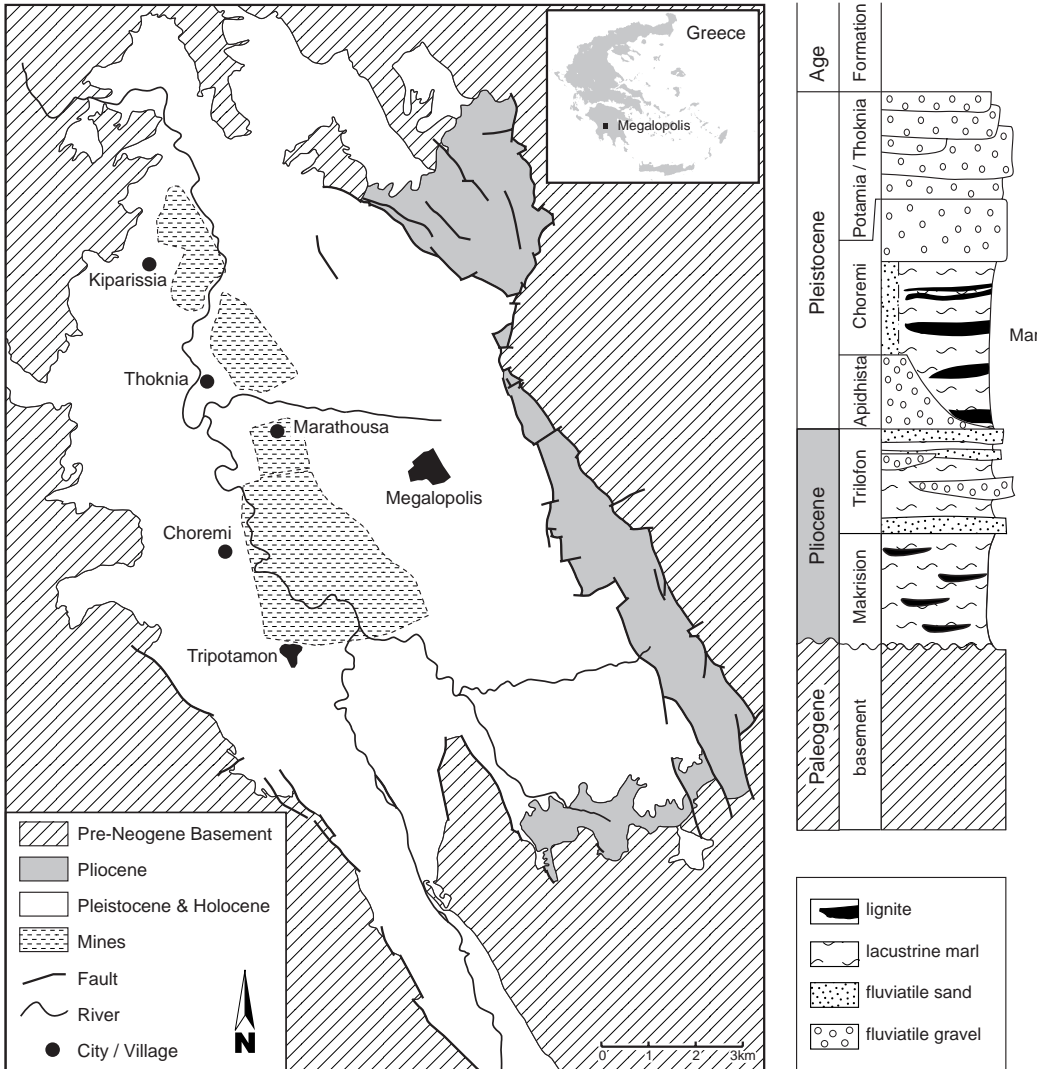


Figure 1: Geological sketch map of the Megalopolis basin and stratigraphic column of the basin fill (not to scale).

and become thinner towards the west. This is in accordance with the half-graben configuration of the basin, with major subsidence along the steep faults in the east, providing accommodation space for the abundant detrital sediment from the steep relief. Along the western margin, where subsidence was moderate, the lake bottom dipped gently, enabling swamps to accumulate organic material for prolonged periods of time. The northernmost mine, the Kiparissia field, is closest to the western margin of the basin. Here, the Marathousa Member is represented by a single massive lignite without detrital interbeds.

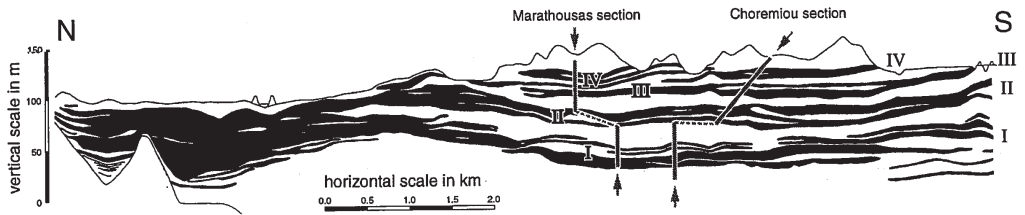


Figure 2: Schematic cross section through the Megalopolis basin. Roman numerals indicate the major coal seams, arrows indicate the positions of the two samples sections.

Vertebrate remains from the Marathousa Member

The occurrence of mammalian fossils in deposits exposed in the Megalopolis Basin has been mentioned in several papers published in the 19th century or in the first half of the 20th century. Melentis described the Pleistocene larger mammal remains excavated from six different localities near the village of Megalopolis in a series of papers (1961; 1963a; 1963b; 1965a; 1965b; 1965c; 1965d; 1965e). The fossils came from six fossiliferous horizons ranging in age from the Early to the Late Pleistocene (Melentis, 1961). The stratigraphical position of these finds is not clear and the faunal data can therefore not be used to date the deposits (Vinken, 1965). In 1962 and 1963 a team of German geologists collected mammal fossils from the Marathousa Beds during a detailed geological survey of the Megalopolis Basin. The faunal remains were described by Sickenberg (1975) who identified eleven species of larger mammals (carnivores, *Mammuthus meridionalis*, *Hippopotamus antiquus*, four different cervids including *Praemegaceros verticornis*, a water buffalo, a horse and *Stephanorhinus etruscus*). He referred the fauna to the Early Biharian. A remarkable specimen in the fossil assemblage from the Marathousa Member is an upper M₃ of a hominid. The oldest evidence for the presence of hominids in Europe, according to Sickenberg (1975).

Sickenberg's opinion about the stratigraphical position of the Marathousa Member was modified by Benda et al. (1987), who assumed a late Villanyian age for the lower lignite bed exposed in the Thoknia open cast lignite mine, on the basis of its smaller mammals. In the early eighties, de Bruijn and van der Meulen took samples from four levels in the same mine (Thoknia 1-4), all these yielded an unpublished, small collection of fossil

	CHO 1	CHO 2	CHO 3	CHO 4
Pisces (Cyprinidae)	x	x	x	x
Aves indet.			4	1
Amphibia:				
<i>Rana (ridibunda)</i> sp.		11	42	11
Reptilia:				
<i>Emys orbicularis</i>		3	9	5
cf. <i>Coronella austriaca</i>			1	
<i>Elaphecf. E. longissima</i>			1	
<i>Natrix</i> sp.		47	94	40
<i>Natrix natrix</i>		2		2
<i>Vipera berus</i> group				1
Mammalia:				
Soricidae indet.	1			1
<i>Castor fiber</i>		1	12	1
<i>Sciurus</i> cf. <i>Vulgaris</i>			1	
<i>Pliomys</i> aff. <i>episcopalis</i>			4	
<i>Miomys</i> aff. <i>savini</i>	30	30	43	36
<i>Miomys</i> sp.		1		1
<i>Apodemus</i> cf. <i>sylvaticus</i>			1	
<i>Apodemus</i> sp.				15
<i>Mus</i> cf. <i>spretus</i>				39
<i>Mus</i> sp.			1	
Muridae gen. et p. indet.			1	
Mustelidae indet.	1		1	
<i>Hippopotamus</i> sp.			1	
Cervidae indet.			3	1

Table 1: List of taxa represented in the levels CHO 1, 2, 3 and 4 and the number of specimens. Please note that the fauna CHO 1 has not yet been investigated for the presence of amphibians and reptiles.

vertebrates. The Marathousa Member was sampled again for mammalian remains in the Choremiou section in 1995 by Doukas, Theocharopoulos and de Bruijn to contribute to the discussion on the stratigraphical position. Six hundred kg of matrix was screen washed from four different levels with mammalian remains; the two lowermost faunas (CHO 1 and CHO 2) come from lignite I, CHO 3 from the base of lignite II and CHO 4 from lignite III (Figure 6). The samples are rich in both botanical and faunal remains; mammalian fossils are, however, not very abundant. The identified specimens from the four levels are listed in Table 1.

Fish remains such as pharyngeal teeth of carp-like fish (Cyprinidae) are numerous in the four different levels. The bird remains (referred to as Aves indet.) represent various species which clearly differ in size. Frogs, turtles and snakes are most abundant among the herpetofauna of CHO 2, 3 and 4 (Holman & Van Kolfshoten, in prep.). Insectivore remains are rare; in the assemblage CHO 1 there is only the labial part of an upper P4 dext. and in CHO 4 a lower m2 dext. Both specimens closely resemble the

corresponding elements of the living *Crocidura suaveolens*. The beaver teeth from Choremi are rather small in comparison to the living north European *Castor fiber*, but hardly differ from those from the Middle Pleistocene of Mauer (Germany) (Mai, 1979).

Voles

There are three different voles represented in the Choremi faunas. *Pliomys* aff. *episcopalis*, characterized by rooted, high crowned molars and by the absence of crown-cementum in the re-entrant angles occurs only in fauna CHO 3. The occlusal pattern of the *Pliomys* molars (Plate 1: Figure 1a) as well as the height of the enamel free areas (Plate 1: Figure 1b) resembles that of *Pliomys episcopalis*. The molars are, however, larger than the type material from Betfia (length m1 from CHO 3 3.04 – 3.15, length of m1 from Betfia + 2.8 mm.). Other *Pliomys* species such as *Pl. simplicior* and *Pl. hollitzeri* are smaller. The large size of the molars from CHO 3 assigned to *Pliomys* aff. *episcopalis* may be an endemic feature.

A large vole characterized by high-crowned molars with roots and crown-cementum in the salient angles is the most abundant vole in all four assemblages. The upper M3 and the lower m1 do not show the presence of a *Mimomys* islet; one molar shows the presence of a *Mimomys* ridge (which disappears towards the base of the crown). The molars show a negative enamel differentiation. In size the m1 is similar to *M. ostramosensis* (Table 2); the morphology of the M3 from Choremi, however, differs (Plate 1: Figure 2). The molars have a much deeper posterior lingual re-entrant angle which results in two isolated triangles. The posterior dentine triangle of the upper M3 of *M. ostramosensis* is broadly confluent with the posterior loop.

Another large vole is *Mimomys rex*. Characteristic for this species is the morphology of the anteroconid with a deep lingual as well as buccal re-entrant angle. The occlusal pattern of most of the teeth from Choremi does not show these characteristics. The buccal re-entrant angle of these molars is very shallow, the lingual angle is more prominent (Plate 1: Figure 3) but still less well-developed than in the molars of *Mimomys rex*. However, in CHO 2 and CHO 4 there are a few molars with better developed re-entrant angles in the anteroconid (Plate 1: Figure 4). These molars resemble the molars from Thoknia, described and figured by Benda et al. (1987). They assigned the specimens from Thoknia to *Mimomys rex* because of their large dimensions and the morphology of the anteroconid. In the assemblages from Choremi, only a minority have this morphology; the occlusal pattern of most of the larger m1 resembles that of *Mimomys*

	N	range	X
CHO 1	4	3.45 - 3.82	3.68
CHO 2	2	3.61 - 3.67	3.64
CHO 3	6	3.38 - 4.01	3.74
CHO 4	2	3.34 - 3.40	3.37

Table 2: Length of the m1 of *Mimomys* aff. *savini* from CHO 1-4.

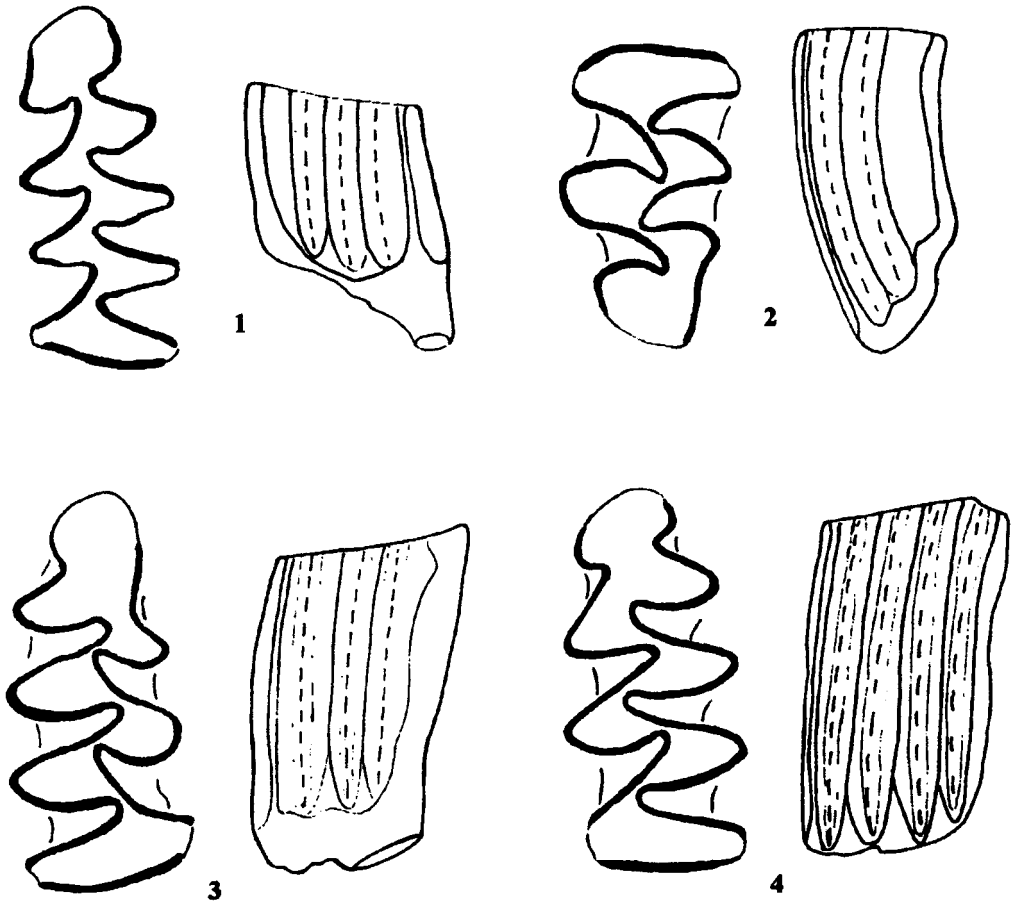


Plate 1: Voles from Choremi (Megalopolis Basin, Peloponnesos). Figure 1: *Pliomys* aff. *episcopalis* m1 sin. (Ch 3-39); Figure 2-4: *Mimomys* aff. *savini*; Figure 2: M3 sin. (Ch 1-23); Figure 3: m1 dext. (Ch 3-31); Figure 4: m1 sin. (Ch 2-31). a: occlusal surface; b: lingual view. All figures approximately x25

savini. The Choremi molars are, however, larger than the type material of *M. savini* from West Runton (England) (length m1: 3,08 – 3,56 mm; x 3.33 mm) (Table 2). Because of the large size of the molars we prefer to assign the material to *Mimomys* aff. *savini*, assuming that the larger voles represent a single species. We include the *Mimomys rex* morphotypes into the population of *Mimomys* aff. *savini*. A medium-sized *Mimomys* species could be identified in the assemblages CHO 2 (M1) and CHO 4 (m2). These two molars have a *Mimomys* pattern, are rooted and show the presence of crown-cementum in the re-entrant angles. They are, however, too small to be assigned to *Mimomys* aff. *savini*.

Mus

The isolated cheek teeth of a species of *Mus* from Choremi are morphologically and metrically similar to extant *Mus spretus* (Plate 2, Table 3). similar teeth are present in the uppermost sample taken from the Thoknia section (Th 4) and in the associations collected from the base of cycle II (CHO 3) and from the lignite of cycle III (CHO 4). This suggests that the immigration of this species is documented within the Marathousa member. The main interest of these occurrences is that they date the FAD of *Mus* in Greece between 700 and 750 thousand years before present (see cyclo-magnetostratigraphic discussion below). This is considerably later than the first record of the genus in N. Africa (Pliocene of Ichkeul, (Jaeger, 1975)), but may be roughly coeval with the oldest known occurrences from the Carpathian basin (Tarkö; Janossy, 1986) and from the South of France (Le Vallonet; Chaline, 1971).

Tooth position	Species	Length		N	Width	
		range	mean		mean	range
M1	<i>Mus spretus</i> (extant)	16.8-19.0	18,2	12	11,1	10.5-11.6
	<i>Mus cf. spretus</i> (TH 4)	16.9-18.3	17,8	3	11,1	10.8-11.6
	<i>Mus cf. spretus</i> (CHO 4)	17.9-18.5	18,1	–	10,5	10.2-10.8
M2	<i>Mus spretus</i> (extant)	9.5-11.8	11	12	10	8.0-10.7
	<i>Mus cf. spretus</i> (TH 4)	10.3-11.6	10,9	4	10,1	10.0-10.2
	<i>Mus cf. spretus</i> (CHO 4)	22.0-12.0	11,4	5	9,8	9.7-10.0
M3	<i>Mus spretus</i> (extant)	5.9-7.0	6,6	4	7,3	6.8-7.5
	<i>Mus cf. spretus</i> (TH 4)	- -	--	-	--	- -
	<i>Mus cf. spretus</i> (CHO 4)	- -	6	1	6,3	- -
m1	<i>Mus spretus</i> (extant)	14.8-16.0	15,5	10	9,3	8.8-10.0
	<i>Mus cf. spretus</i> (TH 4)	14.8-15.8	15,3	5	9,4	9.2-9.5
	<i>Mus cf. spretus</i> (CHO 4)	14.7-15.7	15,3	7	9,2	8.9-9.5
m2	<i>Mus spretus</i> (extant)	9.8-11.3	10,4	10	9,1	8.7-9.7
	<i>Mus cf. spretus</i> (TH 4)	10.0-11.4	11	6	9,2	8.7-9.5
	<i>Mus cf. spretus</i> (CHO 4)	9.0-10.9		14	9,2	8.7-9.8
m3	<i>Mus spretus</i> (extant)	6.7-7.9	7,2	5	6,3	6.0-6.8
	<i>Mus cf. spretus</i> (TH 4)	- -	--	-	--	- -
	<i>Mus cf. spretus</i> (CHO 4)	6.7-8.0	7,3	9	6,6	6.3-6.8

Table 3: Length and width of the cheek teeth of extant *Mus spretus* from Paradision (island of Rhodes) and of the Pleistocene material from the Megalopolis Basin (Peloponnesos); TH 4 indicates the sample Thoknia 4 from De Bruijn and Van der Meulen (unpublished), CHO 4 is from this study.

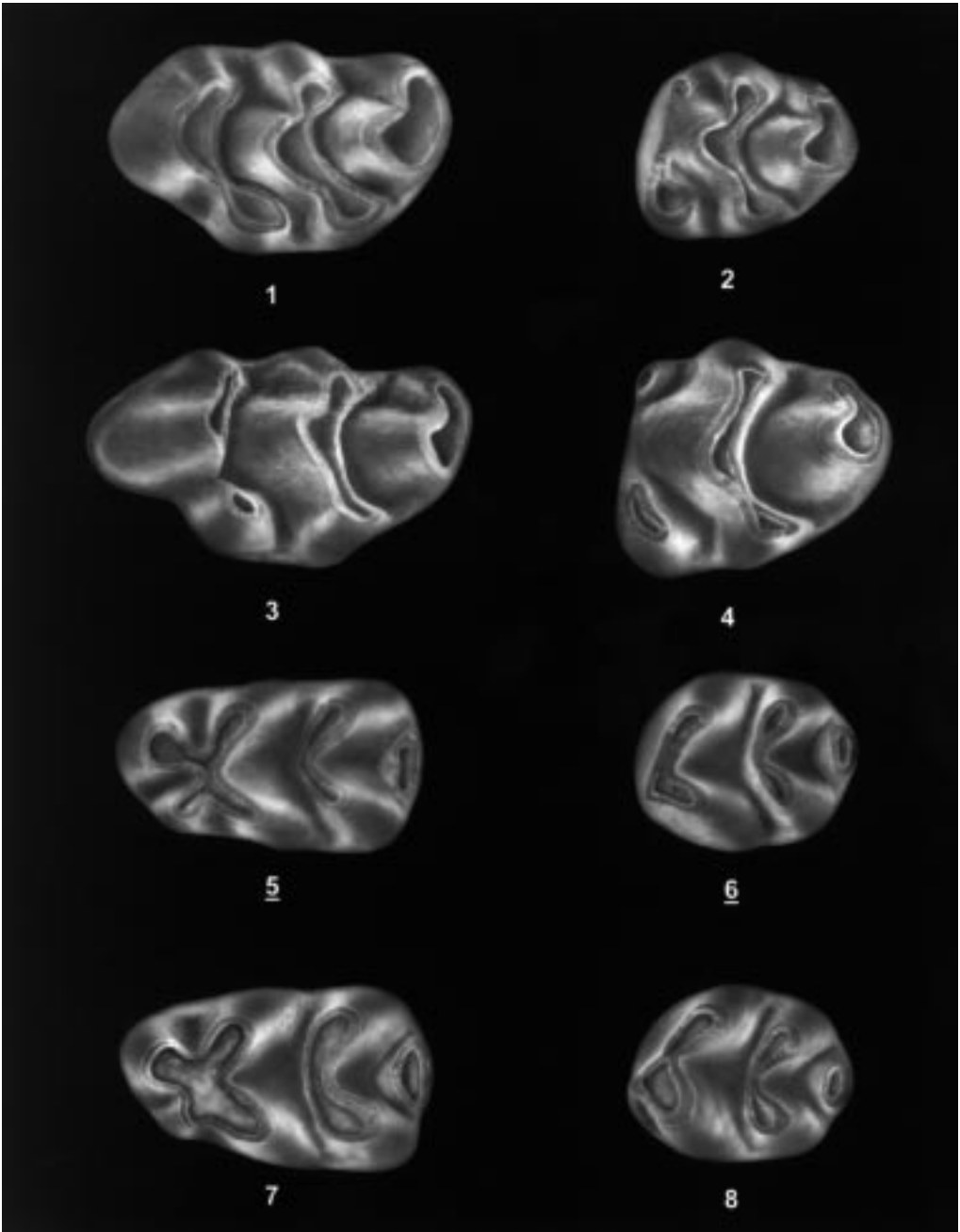


Plate 2: *Mus spretus* from Paradision Rhodes (extant), Figure 1: M1 sin., Figure 2: M2 sin., Figure 5: m1 dext. (reversed), Figure 6: m2 dext. (reversed). *Mus cf. spretus* from CHO 4, Figure 3: M1 sin., Figure 4: M2 sin., Figure 7: m1 sin., Figure 8: m2 sin. All figures approximately x35

Since the dental morphology of different fossil and extant species of *Mus* is very similar, identification of our material to species level would require a detailed analysis of all the material available, a job that is out of the scope of this study (for a review of fossil occurrences of *Mus* see Auffray et al., 1990). Using the criteria that were developed by Darviche and Orsini (1982) on the basis of biochemically screened specimens of *Mus spretus* and *Mus musculus* from the South of France shows that the material from the Megalopolis basin is very similar to extant *Mus spretus*. The only difference detected is that the anterolabial cinquulum of the M2 is better developed in our material than in the reference material of *M. spretus* from the island of Rhodes. We therefore identify the specimens from Megalopolis as *Mus* cf. *spretus*.

Other than the material of *Mus* cf. *spretus* the levels II and IV of the Thoknia section and the levels III and IV of the Choremiou section yielded some isolated cheek teeth of *Apodemus*. Judging by size there seems to be more than one species represented. One *Apodemus* M2 from Th II lacks the t9 entirely and may therefore be referable to *A. maasrichtiensis* (van Kolfschoten, 1985) from the Middle Pleistocene of Maastricht-Belvédère.

Larger mammals

Two fossils (a fragment of an upper M2 in CHO 1 and a lower p3 in CHO 3) indicate the presence of a medium-sized mustelid. *Hippopotamus* sp. is represented by an upper tusk found in CHO 3. Three molar-fragments and an incisor indicate the occurrence of a deer (Cervidae indet.) in size intermediate between the extant roe deer (*Capreolus capreolus*) and the red deer (*Cervus elaphus*).

Environmental conclusions

The mollusc associations from the four samples CHO 1 to 4, identified by W. Kuyper (Leiden University), consist of freshwater species; remarkable is the absence of terrestrial species. The herpetofauna is also dominated by (semi)aquatic species and indicates, just as the mollusc-fauna, a permanent, quiet body of water with abundant aquatic vegetation. Peripheral to the aquatic setting there has been a marshy area with some forest.

(Bio)stratigraphical conclusions

The only species that is well represented in the four Choremi faunal assemblages, *Mimomys* aff. *savini*, does not show any difference in morphology or size between different levels, suggesting that the four faunas do not differ much in age. This supports the assumption that there is no major stratigraphical hiatus in the Choremiou sequence. The biostratigraphical position of the four faunal assemblages is, however, not very clear. The biostratigraphically important genus *Microtus* is absent and the other voles are difficult to identify with certainty since we most probably deal with populations with some endemic characteristics. The genus *Mus*, occurring in the in the uppermost assemblages (CHO 3 and 4), however, indicates that, for the upper part of the sequence, we are dealing with Late Biharian deposits. *Mus* appears in Central Europe during the Middle Pleistocene; since the genus is known from Late Biharian faunas such as Tarkö and Le Vallonet.

Mus cf. spretus is also present in the fauna Thoknia 4 together with the Late Biharian *Microtus arvalidens*. Based on the assumed continuity in the section we conclude that the entire Marathousa Member either dates from the Late Biharian, or that the lower part of the sequence has a late Early Biharian and the upper part a Late Biharian age. This conclusion slightly modifies earlier (bio)stratigraphical correlations, in particular that published by Benda et al. (1987). They assume a Late Villanyian age for the Marathousa Member because of the presence of *Mimomys rex* and the absence of *Microtus* in the fauna from the lower part of the Thoknia sequence. The assignment of the larger voles to *Mimomys rex* has been questioned above. What remains is the absence of *Microtus*. It is important to realize that the number of specimens is restricted and that there are only three species of voles represented in the fauna. This might explain the absence of the genus *Microtus*. However, there might be a taphonomical explanation. The complete absence of terrestrial molluscs in the faunas CHO 1 to 4 and the dominance of aquatic species in the herpetofauna indicate specific environmental conditions, that are unfavorable for the terrestrial voles such as *Microtus*.

Sickenberg's (Sickenberg, 1975) conclusion that the Marathousa Member dates from the Early Biharian is based on the correlation between the larger mammal fauna from the Megalopolis Basin and other European faunas with an Early or Middle Pleistocene age. The Biharian is a biozone based on smaller mammals. The correlation of the smaller mammal biozonation to the larger mammal biozonation is still unsatisfactory, which makes a correlation of a larger mammal fauna to the smaller mammal biozonation problematic in some cases. Moreover, Sickenberg's definition of the Biharian differs from the original definition used by e.g. Kretzoi (1965) and van der Meulen (1973). Faunas with an early Middle Pleistocene age (e.g. Voigtstedt) date, according to Sickenberg (1975), to the Early Biharian. This indicates that there is no contradiction between Sickenberg's and our results.

On the basis of the mammalian record, the sedimentary cycles II and III have a Late Biharian age and cycle I with the faunas CHO 1 and CHO 2 is only slightly older and has a late Early Biharian or a Late Biharian age. This conclusion confirms that the palaeomagnetic reversal indicated in deposits in between cycle I and II can be correlated with the Matyama/Brunhes transition.

Palaeomagnetic sampling and laboratory methods

Two sections were sampled for palaeomagnetic analysis: one in the Marathousas mine, and a second one in the Choremiou mine. The Marathousas section begins at the base of lignite I and ends 65 m higher, above a series of dark clay bands overlying lignite IV (Figures 2 and 4a). The sample spacing in this first section was ~2 m, with 51 samples in total. The more detailed Choremiou section starts ~20 m below lignite I and ends ~20 m above lignite IV (Figures 2 and 4b). Samples (380 in this section) were generally taken every ~0.4 m, but were as closely spaced as 6 cm in intervals where reversals or excursions were expected (based on the results from the parallel Marathousas section).

An electrical drill was used to take oriented rock samples with a diameter of 2.5 cm. In the laboratory, these cores were cut into specimens with a length of 2.2 cm. The samples below the first lignite were obtained from a vertical core with a diameter of 10 cm, drilled by the Greek national mining company, and could only be oriented in a vertical sense (up/down). Non-lignite lithology was preferred, because pure lignite usually does not give meaningful palaeomagnetic results (van Vugt et al., 1998). Sand occurs often in lenses that incise underlying sediments, so they represent discontinuities in the succession. Therefore, sand was avoided, where possible, by shifting the sampling/logging track sideways. The outcrops in the mines were less than a year old, so digging was hardly necessary to reach the fresh rock. The Marathousas section was primarily logged to enable identification of the sample positions, not for cyclostratigraphic purposes, therefore the presentation of Marathousas shows less detail than that of Choremioiu.

The natural remanent magnetisation (NRM) was measured on a 2G squid cryogenic magnetometer. The non-lignitic samples were thermally demagnetised with temperature increments of 30 and 50°C, up to 600°C. The lignitic samples were progressively demagnetised along three axes in a static alternating field (AF) up to 130 mT. At high alternating fields, the samples acquired a gyroremanent magnetisation (GRM) (Dankers and Zijdeveld, 1981; Stephenson, 1993), concealing the NRM. Therefore, above fields of 50 mT, we followed the method of Dankers and Zijdeveld (1981), in which the samples are initially demagnetised along two orthogonal axes, without measuring residual remanence, followed by demagnetisation along the third orthogonal axis and the first two axes, with measurement of the residual remanence along the demagnetised axis after each treatment.

Cyclostratigraphic frame for the Marathousa member

The lignite occurrences in Megalopolis are concentrated in 10–20 metre-thick seams, which alternate with 12–25 metres-thick layers that contain clay, silt and sand. This alternation is regular in the stratigraphic section as well as in a lateral sense, so we interpreted them as sedimentary cycles (roman numerals I–IV in Figures 2 and 4). The clay-silt-sand sequence between lignites I and II is approximately twice as thick as the other detrital units. Lignite V is very clear, but does not necessarily represent a full cycle, because it is much thinner than the other lignite cycles. Above lignite V, the clay-silt unit is thicker than average. In the top of the Choremioiu section, no cycles could be distinguished above lignite IV, where the sediment contains many small carbonate concretions, and layers are indistinct. The cyclostratigraphy for the upper part is therefore based on the Marathousas section only.

Smaller scale cycles are also present. These are defined by the regular occurrence of lignite or dark brown clay layers in the detrital phase of the larger-scale cycles. These layers are generally made of lignite in the western part of the basin, and pass into thinner and/or less organic layers towards the east. The regularly intercalated and laterally continuous detrital layers in coal seam IV were also interpreted as small-scale cycles. The

small-scale cycles were discovered during the second field study, when the lower half of the Marathousas section could not be reached anymore because of mining activities. Therefore, the cyclic pattern in the detrital layers between I and III is based on the Choremiou section only.

In the detrital unit between I and II, six sub-cycles (a-f) could consistently be distinguished at regular stratigraphic intervals (Figure 6). Cycles a and c have genuine lignite beds; the other cycles are lignitic towards the west, but characteristically consist of dark clay. Cycle f seems thinner than average, but the boundary with the overlying lignite (II) is transitional. The detrital unit between II and III contains one prominent lignite bed, signifying at least one cycle (g), but there might be more cycles present in this unit. Between lignite III and IV, two distinct lignite layers occur (h and j), with h being consistently thinner than j. Lignite j contains a thin tephra layer, thus confirming the cyclostratigraphic correlation between both sections. This tephra layer is in all places located in the top part of the lignite layer, indicating that the lignite-detrital alternations represent synchronous palaeo-environmental changes rather than lateral facies shifts. Above lignite IV, more or less regular lithological alternations exist in the detrital units, but the pattern was not apparent. There generally are three prominent lignites or dark layers that we interpreted as small-scale cycles k, l and m (l might be a large-scale cycle and is also called V). within the lignites I, II and III, there are many interbeds; some of them are lenticular (not drawn in Figure 4), but others are continuous over the length of the outcrop (~3 km). These non-lignite (clay, silt and occasionally marl/carbonate) layers occur irregularly, thus inhibiting cyclic interpretation. Only lignite IV is consistently divided into cyclic parts: the small-scale cycles α , β and γ (Figure 4).

Palaeomagnetic results

The NRM intensities vary between nearly zero and $\sim 10^5 \mu\text{Am}^{-1}$; clay and silt have generally higher intensities than organic-rich lithologies. A small, randomly oriented viscous component is in all cases completely removed at 15 mT or 200°C, and from the samples with reversed polarity it can be seen that there is hardly any present-day-field component present in these unweathered rocks (Figure 3b). The separate-axis measurement method after alternating field demagnetisation removes the largest part of the gyroremanent magnetisation, but directions still tend to move away from the stable (15–50 mT) direction, so some remaining influence cannot be excluded. Therefore, only the data points acquired at fields between 15 and 50 mT are used to obtain the direction of the characteristic remanent magnetisation (ChRM). Thermal demagnetisation also has a limitation, at 390°C. Some samples have reached their maximum unblocking temperature at 390°C, but most were not yet fully demagnetised, while both the intensity and direction of the remanence sometimes showed drastic changes above this temperature. Rock magnetic investigations (van Vugt et al., 2000b) have shown that when the intensity of the characteristic component in samples from Megalopolis is higher than $10^3 \mu\text{Am}^{-1}$, the sample is dominated by secondary greigite. These samples were discarded in

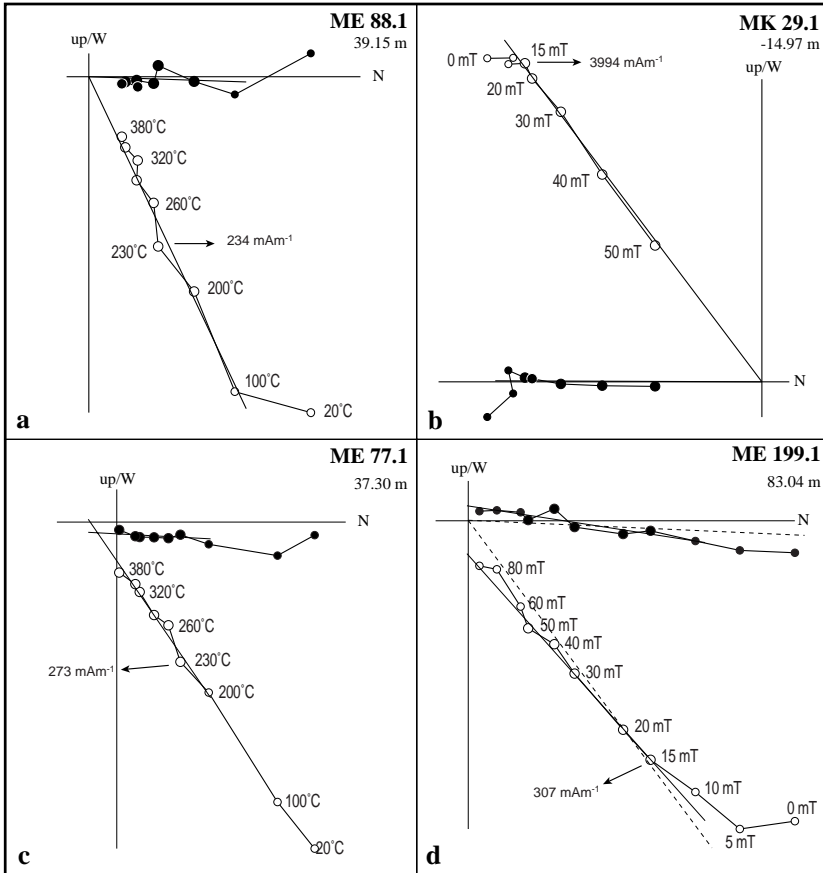


Figure 3: Demagnetisation diagrams Figures a and b show unambiguous normal and reversed polarity, respectively; c is clearly missing the origin, d might pass the origin, but is uncertain.

this study. The samples that were used probably contain a mixture of magnetite and a ferrimagnetic iron sulphide (van Vugt et al., 2000b). Low-intensity data are more sensitive to disturbances. In order to reduce the risk of interpreting noise, the samples with intensities $<100 \mu\text{Am}^{-1}$ were not used for magnetostratigraphy.

The Zijderveld diagrams have been divided into three categories: a line straight towards the origin, either from a reversed or from a normal direction (Figure 3a, b); a line clearly missing the origin (Figure 3c); and an uncertain group (Figure 3d). The samples from the core (between -20 and 0 m) were interpreted based on their inclination only. Interpretation of the samples from the first group was straightforward, and the directions are plotted in Figure 4 as black dots connected with a line. The directions indicated by the straight lines clearly missing the origin were interpreted as secondary, with the primary magnetic polarity being opposite (large white circles). With the great circle

method the primary directions were approximated (large asterisks). The directions calculated from the third group of samples (small grey circles) are considered to be not very reliable, but a great circle analysis was used as a very rough estimation of the possible primary direction (small asterisks).

Discussion

Magnetostratigraphy

Both the Marathousas and Choremiou sections recorded reversed polarity at the base, and normal polarity in the rest of the section (Figure 4). In the Choremiou section there are many samples near the reversal with a normal (low-T/low-Field) component and a probably or possibly reversed primary remanence remaining after 50 mT or 390°C. This indicates that (part of) the magnetic remanence was acquired some time after deposition. This delayed acquisition causes the position of a polarity reversal to be at least as high as the highest sample that recorded the pre-reversal polarity. The position of the reversed-to-normal polarity transition in this section is therefore at least higher than 23 m, but there is a single, possibly reversed sample at 37.3 m (ME 77, see Figure 3c). This could be an indication for a reversal excursion, but remanence acquisition is so much delayed that the chance of recording a very short polarity event is negligible. We therefore regard the polarity between 23 and 38 m (lower half of the detrital interval above lignite I) to be uncertain. In the Marathousas section, there are no indications for reversed polarity above 12 m (middle of lignite I), but the sample spacing was much larger. These two sections are exactly parallel, so, according to the principle of delayed acquisition, the reversal is positioned at the highest possible level, i.e. the level from the Choremiou section.

Since previous palynological and palaeontological data (Benda et al., 1987; Lüttig and Marinos, 1962; Vinken, 1965) point to a middle Pleistocene age for the studied sediments, the normal interval can theoretically represent the Olduvai, Jaramillo or Brunhes (sub)Chron. The Jaramillo lasts only 80 kyr, the Olduvai 157 kyr. If the normal polarity interval in Megalopolis would represent a part of the Olduvai subchron, the sedimentation rate would be at least 57 cm/kyr, which is extremely high for lignite deposits. Moreover, since the present palaeontological study indicates a late Early Biharian or a Late Biharian age for lignites I and II, the normal interval is considered to represent the lower part of the Brunhes Chron (the only prolonged normal polarity period in the Pleistocene), and the recorded reversal the Matuyama-Brunhes boundary.

Phase relationship

In their pollen analysis of (the lowermost) lignite I of Megalopolis, Nickel et al. (1996) found the palaeoclimate to change from a temperate intermediate to a (warmer) Mediterranean climate from the base of the lignite upwards, and a possible opposite trend towards the top of lignite I, but their section was too short to certify this last

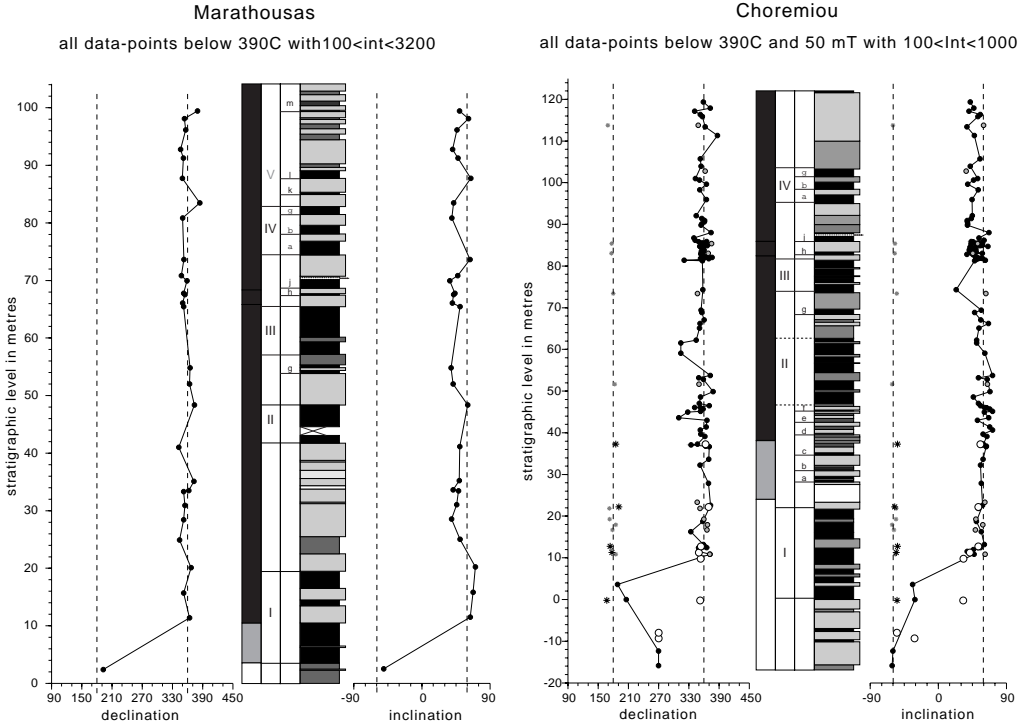


Figure 4: Palaeomagnetic results, polarity zones, large-scale cycles (roman numerals), small-scale cycles (letters) and lithology of the Megalopolis sections. Black dots denote primary magnetic directions; large white circles denote overprinted directions with the primary direction being opposite, asterisks denote approximations of these primary directions derived from the great circle method; small grey circles and asterisks belong to the uncertain group (see text). In the polarity column, black (white) indicates normal (reversed) polarity, while shaded indicates undetermined polarity. In the lithological column, black (shaded) indented beds denote lignite (dark-clay equivalent of lignite), shaded (white) protruding beds denote detrital (sand) layers, and the +++line indicates the position of the volcanic ash layer.

observation. They interpreted a lignite to represent an interglacial or interstadial. In a similar sedimentary setting in Lupoia (Romania) from the lower Pliocene, with more time control points (Radan and Radan, 1996; Radan and Radan, 1998; van Vugt et al., 2000a), the alternation of lignite and detrital beds was found to have an average period of ~100 kyrs, with the lignites corresponding to eccentricity maxima (van Vugt et al., 2000a).

A new palynological study (Okuda, in prep.) in Megalopolis on a 70-metre section that contains lignites II to V shows a typical alternation between *Quercus* (oak) and *Artemisia* pollen (Figure 5). *Artemisia*, indicative for cold and dry conditions, is abundant in the detrital intervals. *Quercus*, representative for a relatively warm and humid climate, occurs mainly in the lignites. The lignite–detrital alternation thus coincides with an alternation between warm/humid and cold/arid climate respectively. This leads

to the interpretation that the lignite seams in Megalopolis represent the warm phase in a cyclically changing climate. These warm periods could be either interglacials or interstadials, as Nickel et al. (1996) suggested already.

Smaller scale cycles may tentatively be recognised in the pollen diagram, but the sample resolution is generally too low to confirm them. Only in the lignite of small-scale cycle g two samples were taken, which both have a high arboreal pollen content, indicating a warm and humid phase. Also within lignite II, where small-scale cycles could not be distinguished in the lithology, there is some suggestion for small-scale cyclicity in the pollen record. At 60 and 53 m, a minor drop in *Quercus* that coincides with a peak in *Artemisia* suggest two short cold and arid periods in an otherwise warm and humid period. Further palynological research on a higher-resolution sample set is needed to confirm these small-scale variations.

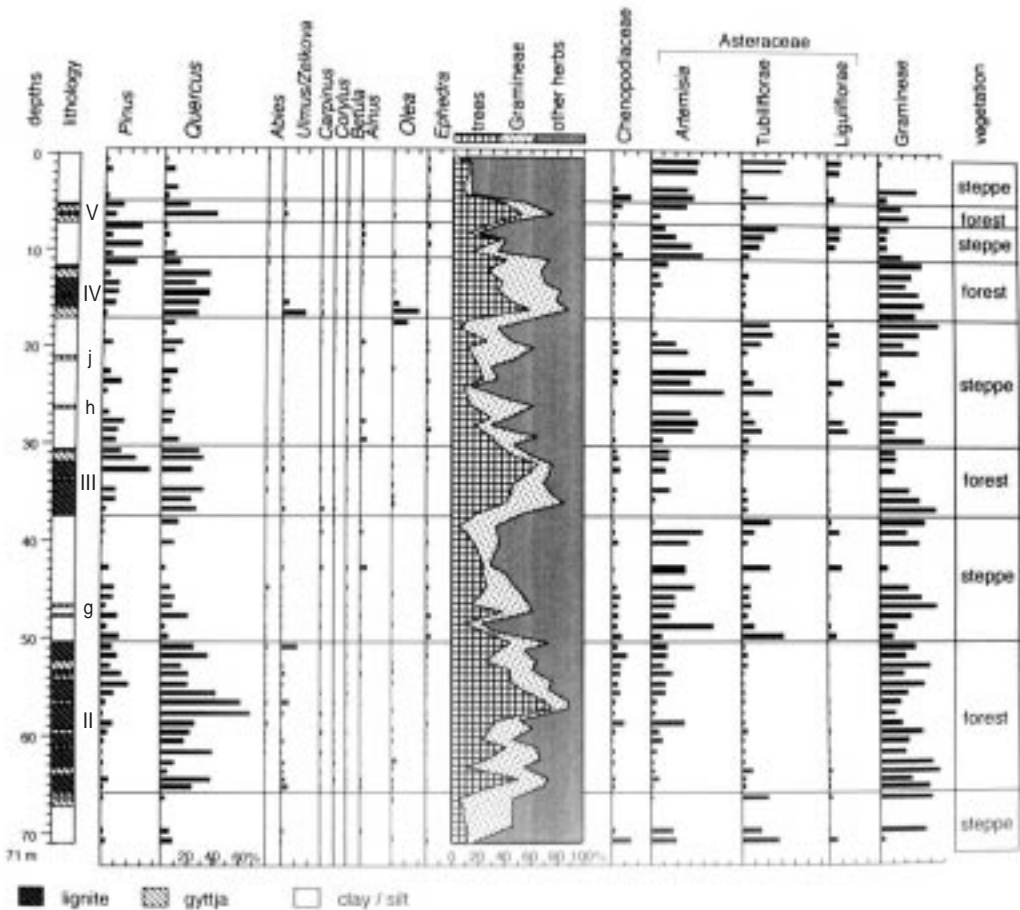


Figure 5: Simplified pollen diagram, after (Okuda, in prep.).

If the large scale cycles represent glacial-interglacial alternations, which would be quite logical considering the regularity and the omnipresent quasi-periodic (~100 kyr) occurrence of ice ages during the late Pleistocene (e.g., Imbrie et al., 1993; Imbrie et al., 1984; Raymo, 1997b and references therein), the average sedimentation rate would be 21 cm/kyr. If, on the other hand, the lignite seams would represent interstadials, which are approximately precession-related (~20 kyr) in the late Pleistocene, the average sedimentation rate would be 105 cm/kyr. This seems too high for such a lacustrine-marsh environment. For comparison, the sedimentation rate in the lignite-carbonate Ptolemais basin (N Greece) is 10 cm/kyr (van Vugt et al., 1998), and in the lignite-clastic Lupoia succession (Romania) it is 18 cm/kyr (van Vugt et al., 2000a). Therefore, we interpret the large-scale cycles to be caused by eccentricity-forced climate changes, and the small-scale cycles to represent precessional cycles. Both types have lignite as the warm/humid phase in the climate cycle, and the detrital beds as the cold/arid phase.

The phase relationship between lithology and astronomical parameters must be established independently and can never be assumed based on the results in other continental basins. This is illustrated by the fact that lignite formation in the Pliocene Ptolemais basin in N. Greece happened during the opposite phase than in Megalopolis, i.e. during insolation minima (cool and dry climate). The carbonate-lignite alternation in Ptolemais is primarily caused by lake level fluctuations as a result of precipitation variations (van Vugt et al., 1998; van Hove, pers. comm.). In other words, when humidity increased, the Ptolemais lake level rose and marsh vegetation drowned, enabling carbonate precipitation to increase; during more arid conditions, the lake level lowered and the lake was overgrown by reed swamp vegetation, creating anoxic conditions in which organic material was preserved. The forcing mechanism for Megalopolis is not clear yet, but a possible explanation is that during cold and dry periods, vegetation around the basin and/or along the lake margins that could trap the sediment was scarce, so erosional products could be transported far into the basin, where they formed the detrital beds. When the climate became warmer and more humid, conditions for vegetation improved, and large quantities of organic material were preserved. Detailed studies (palynology, organic petrology and/or sedimentology) within the current cyclostratigraphic frame will be needed to further test this hypothesis.

Astronomical tuning

Preferred tuning based on the sedimentary pattern

Recognition of the typical pattern caused by superposition of the 400 kyr cycles on 100 kyr-eccentricity would make the presumed relation between the large-scale cycles and eccentricity more credible. The Matuyama-Brunhes boundary is recorded in the extra-thick detrital interval above lignite I. This interval could well correspond to the 400 kyr minimum at 0.78 Ma, around the Matuyama-Brunhes boundary (Figure 6). The regular pattern formed by lignites II-IV and the detrital intervals in-between matches the three prominent eccentricity maxima at 0.7, 0.6 and 0.5 Ma. Lignite I (V) is much thinner,

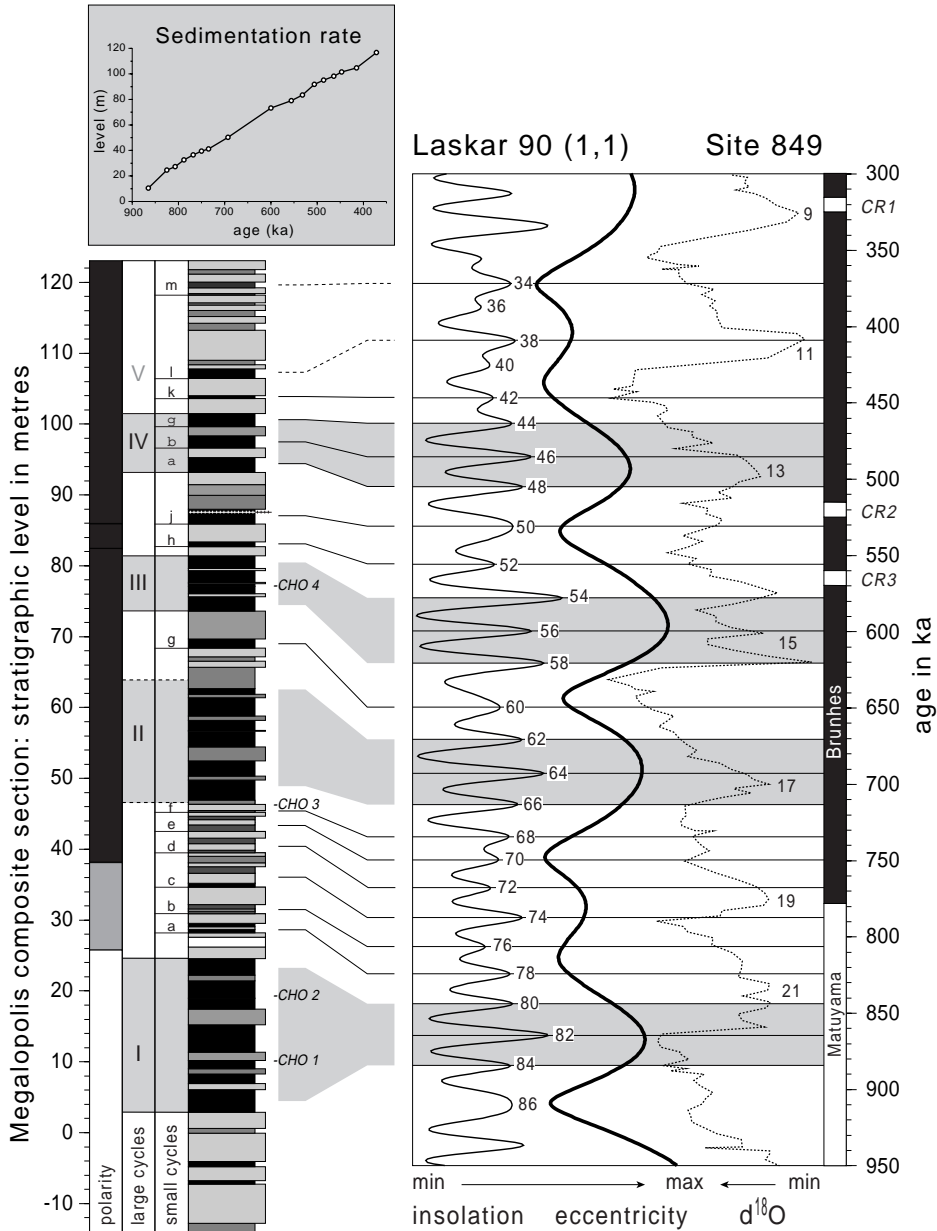


Figure 6

Figure 6: Megalopolis composite section (polarity, cyclostratigraphy and lithology; see also caption to Figure 4) correlated with insolation (i-cycle codification after (Lourens et al., 1996)) and eccentricity (Laskar, 1990). $\delta^{18}\text{O}$ -record from site 849 (Mix et al., 1995; Raymo, 1997a) plotted to the GSS97 timescale (Raymo, 1997b) with selected isotope stages labelled and magnetic polarity timescale with excursions labelled in italics (Langereis et al., 1997). CHO 1-4 indicate small-mammal faunas. Inset: sedimentation rate resulting from this correlation.

which is in agreement with the low-amplitude 100 kyr-maximum at 0.4 Ma. In conclusion, the large-scale coal seam pattern correlates well with the eccentricity pattern between 0.9 and 0.35 Ma.

In the Mediterranean, the best fitting target curve for the Pliocene and Pleistocene is generally considered to be the 65°N summer insolation (average of June and July) as calculated by Laskar (1990), because it best matches the marine geological record (Lourens et al., 1996). The small-scale cycles are correlated to this insolation curve as illustrated in Figure 6. The thick lignitic part of cycle c is correlated with high-amplitude i-cycle 74, and the very thin non-lignitic phase of cycle e is connected to the very low-amplitude insolation minimum 69. The interval between lignites II and III appears to contain only one small-scale cycle (g), that is correlated to long-duration i-cycle 60. Cycles h (thin) and j (thick) are correlated to the consecutive low and relatively high amplitude i-cycles 52 and 50, respectively. I-cycle 50 also has a long duration. In this correlation, the lignite seams are supposed to represent two insolation minima, consistent with the two colder phases observed in the pollen record of lignite II.

The stratigraphic levels of the midpoints of all lignites are plotted versus their astronomically tuned age (Figure 6, inset). The resulting sedimentation rate is fairly constant throughout the section, without any sudden changes or outliers that would imply erosion and major hiatuses.

Alternative tuning based on palynological data

The pollen record of Okuda (in prep.) shows a distinct peak in *Olea* (Olive trees) in three samples around the base of lignite IV. This could be interpreted as a short period that was distinctly warm, and possibly warmer than any other sampled interval. Based on the pollen record alone, it would seem valid to correlate this peak to the warm interglacial stage 11. The consequence of correlating the underlying lignite seams with subsequently older eccentricity maxima or interglacial stages is that the Brunhes–Matuyama boundary below lignite II then has an age that is one cycle too young. This would imply a considerable hiatus in the record, which is of course possible in a continental environment. The most likely position for such an unconformity would be the lower boundary of lignite II. This boundary is formed by an irregular transition zone that is locally cut by the overlying lignite. The rich CHO 3 fauna was found in this transition zone, indicating a, possibly prolonged, period of non-deposition.

Correlation of the sedimentary cycles with the insolation curve – based on the assumption that one large-scale cycle is missing below lignite II – does neither result in a good fit for the small-scale cycles g–j, nor for the cycles α – γ . Therefore, the first correlation is preferred.

Consequences

The details in the pattern of lignites and lignite seams matches very well with the astronomical target curves of insolation and eccentricity. The correlation with $\delta^{18}\text{O}$ curves or stacks (Bassinot et al., 1994; Imbrie et al., 1984) or ice volume curves (Imbrie and Imbrie, 1980; Paillard, 1998), however, reveals some important differences (Figure 6).

We compare the Megalopolis section to the Pacific $\delta^{18}\text{O}$ record from ODP core 849, because this is generally considered to be a very detailed record. The critical features are the same in all marine $\delta^{18}\text{O}$ records, including those from the Mediterranean Sea. Prominent interglacial stage 19 (~780 ka) is not represented by a prominent lignite in Megalopolis (interval between lignite I and II). The same holds for stage 11 and corresponding lignite V. Stage 17 (~680 ka) is significantly less pronounced than stage 15 (~600 ka) in the $\delta^{18}\text{O}$ records, whereas the corresponding lignites (II and III, respectively) show hardly any difference within the width of the outcrops (~3 km). Apparently, the pattern of lignite seams in Megalopolis was forced by eccentricity and not by (whatever forced) the glacial-interglacial cycles as recorded in the world oceans by stable oxygen isotopes.

The oxygen isotope variations in the world oceans are mainly a reflection of the global ice volume. Isotope records from the Mediterranean basin document regional climate changes superimposed on the global signal. The much higher amplitude of $\delta^{18}\text{O}$ variations in Mediterranean records is associated with reduction in surface-water salinity as a regional response to global increase in ice volume and decrease of temperature (Ganssen and Troelstra, 1987; Howell et al., 1998; Thunell et al., 1990; Vergnaud-Grazzini et al., 1986; Williams et al., 1978, among others). Apart from differences in amplitude, the Mediterranean isotope records of Sites 963, 964 and 967 from the eastern Mediterranean are comparable with oceanic oxygen isotope records at the critical stages 19 and 11 (Howell et al., 1998; Kroon et al., 1998). So, either the forcing of the regional (continental) Mediterranean climate was different from the eccentricity forcing of the lignite pattern in Megalopolis, or, more probably, the Mediterranean marine isotope records are influenced more by global factors than by regional climate.

Conclusions

The Megalopolis section is dated as Pleistocene with magnetostratigraphy (lower Brunhes) and palaeontology (Late Biharian). Subsequent astronomical tuning of the lignite pattern gave ages of ~900 ka for the base of the section and ~350 ka for the top. Each lignite seam represents an eccentricity maximum, individual lignites represent insolation maxima. Not all the astronomical cycles are recognised in the lithology. Most notable is that low-amplitude eccentricity maxima lack expression as lignite seams, although they are recorded as normal interglacial stages in the marine oxygen isotope records (from both the Mediterranean Sea and the open oceans). Apparently, the regional Mediterranean climate was either forced by a different mechanism than the one determining the lignite–detrital alternations in Megalopolis, or the Mediterranean marine isotope records are influenced much more by global factors than by the regional climate.

Acknowledgements

Dr. Masaaki Okuda from Japan courteously provided his palynological data and scientific opinions. We thank him for his permission to use them in this thesis. This research was much advanced by the fruitful discussions with Joris Steenbrink and Christian Mulder. Field assistance by Joris Steenbrink, Erik Snel, Marloes van Hoeve, Hendrik-Jan Bosch, Johan Meulenkamp, Constantin Doukas, Constantin Theocharopoulos and several Greek miners was much appreciated. The co-operation of the Greek Public Power company (AEI) was essential for collecting our samples. The investigations were supported by the Netherlands Council for Earth and Life Sciences (ALW), part of the Netherlands Science Foundation (grant to NvV). This work was conducted under the programme of the Dutch Vening Meinesz Research School of Geodynamics (VMSG).

References

- Abdul Aziz, H., Hilgen, F.J., Krijgsman, W., Sanz-Rubio, E. and Calvo, J.P., 2000. Astronomical forcing of sedimentary cycles in the Miocene continental Calatayud Basin (NE Spain). *Earth and Planetary Science Letters*, in press.
- Auffray, J.-C., Vanlerberghe, F. and Britton-Davidian, J., 1990. The house mouse progression in Eurasia: a palaeontological and archaeozoological approach. *Biol. Journ. of the Linnean Society* 41, 13-25.
- Bassinot, F.C. et al., 1994. The astronomical theory of climate and the age of the Brunhes-Matuyama magnetic reversal. *EPSL* 126, 91-108.
- Benda, L., van der Meulen, A.J., Meyer, K.J. and van de Weerd, A., 1987. Biostratigraphic correlations in the Eastern Mediterranean Neogene: 8. Calibration of sporomorph- and rodent-associations from the Megalopolis Basin (Peloponnesus, Greece). *Newsl. Stratigr.* 17, 129-141.
- Chaline, J., 1971. La microfaune du Vallonet (A.-M.) et le problème des corrélations micromammifères à la limite Pleistocène inférieur-moyen. *Bulletin du Musée d'Anthropologie Préhistorique de Monaco* 17, 65-69.
- Dankers, P.H.M. and Zijdeveld, J.D.A., 1981. Alternating field demagnetization of rocks, and the problem of gyromagnetic remanence. *Earth and Planetary Science Letters* 53, 89-92.
- Darviche, D. and Orsini, P., 1982. Critères de différenciation morphologique et biométrique de deux espèces de souris sympatriques: *Mus spretus* et *Mus musculus domesticus*. *Mammalia* 46, 205-217.
- Ganssen, G.M. and Troelstra, S.R., 1987. Paleoenvironmental change from stable isotopes in planktonic foraminifera from Eastern Mediterranean sapropels. *Marine Geology* 75, 210-218.
- Howell, M.W. et al., 1998. Stable isotope chronology and paleoceanographic history of Sites 963 and 964, Eastern Mediterranean Sea. *Proceedings of Ocean Drilling Program, Scientific Results* 160, 167-180.
- Imbrie, J. et al., 1993. On the structure and origin of major glaciation cycles, 2, The 100,000-year cycle. *paleoceanography* 8, 699-735.
- Imbrie, J. et al., 1984. The orbital theory of Pleistocene climate: support from a revised chronology of the marine $\delta^{18}\text{O}$ record. In: A. Berger, J. Imbrie, J. Hays, G. Kukla and B. Saltzman (Eds.), *Milankovitch and climate, part I*, pp. 269-305, Plenum Reidel, Dordrecht.
- Imbrie, J. and Imbrie, J.Z., 1980. Modeling the climatic response to orbital variations. *Science* 207, 943-953.
- Jaeger, J.J., 1975. The mammalian faunas and hominid fossils of the Middle Pleistocene of the Maghreb. In: K.W.

- Butzer and G.U. Isaac (Eds.), *After the Australopithecines.*, pp. 399-418.
- Janossy, D., 1986. Pleistocene Vertebrate Faunas of Hungary. *Elsevier Science Publishers.*
- Kretzoi, M., 1965. Die Nager und Lagomorphen von Voigtstedt in Thüringen und ihre chronologische Aussage. *Paläont. Abh.* 2, 587-660.
- Krijgsman, W., Langereis, C.G., Daams, R. and van der Meulen, A.J., 1994. Magnetostratigraphic dating of the middle Miocene climate change in the continental deposits of the Aragonian type area in the Calatayud-Teruel basin (Central Spain). *Earth and Planetary Science Letters* 128, 513-526.
- Kroon, D. et al., 1998. Oxygen isotope and sapropel stratigraphy in the eastern Mediterranean during the last 3.2 million years. Proceedings of the Ocean Drilling Program, *Scientific Results* 160, 181-189.
- Langereis, C.G., Dekkers, M.J., de Lange, G.J., Paterne, M. and van Santvoort, P.J.M., 1997. Magnetostratigraphy and astronomical calibration of the last 1.1 Myr from an eastern Mediterranean piston core and dating of short events in the Brunhes. *Geophysical Journal International* 129, 75-94.
- Laskar, J., 1990. The chaotic motion of the solar system: A numerical estimate of the size of the chaotic zones. *Icarus* 88, 266-291.
- Löhnert, E. and Nowak, H., 1965. Die Braunkohlenlagerstaette van Khoremi im Becken von Megalopolis/Peloponnes. *Geologisches Jahrbuch* 82, 847-867.
- Lourens, L.J. et al., 1996. Evaluation of the Plio-Pleistocene astronomical timescale. *paleoceanography* 11, 391-413.
- Lüttig, G.W. and Marinos, G., 1962. Zur Geologie des neuen Griechischen Braunkohlen-Lagerstaette von Megalopolis. *Braunkohle* 14, 222-231.
- Mai, H., 1979. Die Biberarten Castor und Trogontherium aus den altpleistozänen Schichten von Mauer an der Elsenz. *Schr. Naturw. Ver. Schlesw.-Holst.* 49, 35-46.
- Melentis, J.K., 1961. Die Dentition der pleistozänen Proboscidiere des Beckens von Megalopolis im Peloponnes (Griechenland). *Ann. Géol. d. Pays Helléniques* 12, 153-262.
- Melentis, J.K., 1963a. Die Osteologie der pleistozänen Proboscidiere des Beckens von Megalopolis im Peloponnes (Griechenland). *Ann. Géol. d. Pays Helléniques* 14, 1-107.
- Melentis, J.K., 1963b. Über Equus abeli aus dem Mittelpleistozän des Beckens von Megalopolis im Peloponnes (Griechenland). *Ann. Géol. d. Pays Helléniques* 16, 507-519.
- Melentis, J.K., 1965a. Die pleistozänen Cerviden des Beckens von Megalopolis im Peloponnes (Griechenland). *Ann. Géol. d. Pays Helléniques* 16, 1-92.
- Melentis, J.K., 1965b. Studien über fossile vertebraten Griechenlands. 4. Die pleistozänen Nashörner des Beckens von Megalopolis im Peloponnes (Griechenland). *Ann. Géol. d. Pays Helléniques* 16, 363-402.
- Melentis, J.K., 1965c. Studien über fossile vertebraten Griechenlands. 5. Über Hippopotamus antiquus Desmarest aus dem Mittelpleistozän des Beckens von Megalopolis im Peloponnes (Griechenland). *Ann. Géol. d. Pays Helléniques* 16, 403-435.
- Melentis, J.K., 1965d. Studien über fossile vertebraten Griechenlands. 6. Sus scrofa L. aus dem Jungpleistozän des Beckens von Megalopolis im Peloponnes (Griechenland). *Ann. Géol. d. Pays Helléniques* 16, 436-445.
- Melentis, J.K., 1965e. Studien über fossile vertebraten Griechenlands. 7. Die Boviden des Jungpleistozäns des Beckens von Megalopolis im Peloponnes (Griechenland). *Ann. Géol. d. Pays Helléniques* 16, 446-472.
- van der Meulen, A.J., 1973. Middle Pleistocene Smaller Mammals from the Monte Peglia (Orvieto, Italy) with Special Reference to the Phylogeny of Microtus (Arvicolidae, Rodentia). *Quaternaria* XVII, 1-144.
- Mix, A.C., Le, J. and Shackleton, N.J., 1995. Benthic foraminiferal stable isotope stratigraphy of Site 846: 0-1.8 Ma. *Proc. Ocean Drill. Program, Sci. Results* 138, 839-854.
- Nickel, B., Riegel, W., Schonherr, T. and Velitzelos, E., 1996. Environments of coal formation in the Pleistocene

- lignite at Megalopolis, Peloponnesus (Greece) - reconstruction from palynological and petrological investigations. *N. Jb. Geol. Palaont. A.* 200, 201-220.
- Paillard, D., 1998. The timing of Pleistocene glaciations from a simple multiple-state climate model. *Nature* 391, 378-381.
- Radan, S. and Radan, M., 1996. Magnetostratigraphy as a technique of nomination and correlation of coal beds: two examples from western Dacic basin (Romania). *Geologica Carpathica* 47, 174-176.
- Radan, S.C. and Radan, M., 1998. Study of the geomagnetic field structure in the tertiary in the context of magnetostratigraphic scale elaboration. I - the Pliocene. *Anuarul Institutului Geologic al Romaniei* 70, 215-231.
- Raymo, M.E., 1997a. Major Climate Terminations Data. *IGBP PAGES/World Data Center-A for Paleoclimatology Data Contribution Series # 97-024*.
- Raymo, M.E., 1997b. The timing of major climate terminations. *paleoceanography* 12, 577-585.
- Sickenberg, O., 1975. Eine Säugetierfauna des tieferen Biharium aus dem Becken von Megalopolis (Peloponnes, Griechenland). *Ann. Géol. d. Pays Helléniques* 27, 25-73.
- Steenbrink, J., van Vugt, N., Hilgen, F.J., Wijbrans, J.R. and Meulenkamp, J.E., 1999. Cyclostratigraphy and $^{40}\text{Ar}/^{39}\text{Ar}$ dating of lower Pliocene lacustrine sequences of the Ptolemais Basin, NW Greece. *Palaeogeography, Palaeoclimatology, Palaeoecology* 152, 283-303.
- Stephenson, A., 1993. Three-axis static alternating field demagnetization of rocks and the identification of natural remanent magnetization, gyroremanent magnetization and anisotropy. *Journal of geophysical research* 98, 373-381.
- Thunell, R., Williams, D., Tappa, E., Rio, D. and Raffi, I., 1990. Pliocene-Pleistocene stable isotope record for Ocean Drilling Program Site 653, Tyrrhenian Basin: implications for paleoenvironmental history of the Mediterranean Sea. *Proceedings ODP, Scientific Results* 107, 387-399.
- van Kolfschoten, T., 1985. The Middle Pleistocene (Saalian) and Late Pleistocene (Weichselian) mammal faunas from Maastricht, Belvédère (Southern Limburg, The Netherlands). *Med. Rijks Geol. Dienst* 39, 45-74.
- van Vugt, N., Langereis, C.G. and Hilgen, F.J., 2000a. Dominant expression of eccentricity versus precession in the lithology of Mediterranean continental (lacustrine) deposits. *Geological Utrajectina* 189, Chapter 4.
- van Vugt, N., Langereis, C.G. and Dekkers, M.J., 2000b. Rock-magnetic properties of lignite-bearing lacustrine sediments from the Megalopolis and Ptolemais Basins as possible climate proxies. *Geologica Utrajectina* 189, Chapter 7.
- van Vugt, N., Steenbrink, J., Langereis, C.G., Hilgen, F.J. and Meulenkamp, J.E., 1998. Magnetostratigraphy-based astronomical tuning of the early Pliocene lacustrine sediments of Ptolemais (NW Greece) and bed-to-bed correlation with the marine record. *Earth and Planetary Science Letters* 164, 535-551.
- Vergnaud-Grazzini, C., Devauz, M. and Znaidi, J., 1986. Stable isotope "anomalies" in Mediterranean Pleistocene records. *Mar. Micropaleontol.* 10, 35-69.
- Vinken, R., 1965. Stratigraphie und Tektonik des Beckens von Megalopolis (Peloponnes, Griechenland). *Geologisches Jahrbuch* 83, 97-148.
- Williams, D.F., Thunell, R.C. and Kennett, J.P., 1978. Periodic freshwater flooding and stagnation of the eastern Mediterranean Sea during the late Quaternary. *Science* 201, 252-254.